SENSITIVITY ANALYSIS ON FATIGUE DAMAGE OF CEMENTED HIP PROSTHESES

P. Colombi[1], K. Dolinski[2]

[1]*Department of Structural Engineering, Milan Technical University, Milan, Italy*
[2]*Centre of Mechanics, Institute of Fundamental Technological Research, Warsaw, Poland*
e-mail: colombi@stru.polimi.it

Abstract

In this paper a sensitivity analysis is performed on a finite element model previously developed to study the fatigue behaviour of cemented hip prostheses. The proposed method is based on a "smeared-crack" technique to simulate the evaluation of the fatigue damage process in the cement mantle. The non-linear and anisotropic behaviour of the material after it is locally cracked is simulated by the finite element code ABAQUSÒ. In this paper the sensitivity of the stem subsidence and damage level in the mantle is studied as function of the cement Young modulus, the stem-cement friction coefficient and the stem Young modulus. Numerical results show a significant sensitivity to variations of the cement Young modulus and stem-cement friction coefficient and a moderate sensitivity to the stem Young modulus.

Sommario

In questa memoria viene effettuato uno studio di sensitività su un modello ad elementi finiti precedentemente sviluppato per l'analisi a fatica di un impianto di protesi d'anca cementato. La metodologia sviluppata si basa su di una tecnica di tipo "smeared-crack" per la simulazione della evoluzione del processo di danneggiamento nel mantello in cemento. Il comportamento non-lineare ed anisotropico del materiale una volta fessurato viene simulato mediante il codice ad elementi finiti ABAQUSÒ. Nel lavoro viene valutata la sensitività del valore di abbassamento dello stelo e del livello di danneggiamento del mantello al variare di alcuni parametri del modello quali modulo elastico del cemento, il coefficiente di attrito stelo-cemento ed il modulo elastico dello stelo. I risultati mostrano una significativa sensibilità al variare del modulo elastico del cemento e del coefficiente di attrito ed una modesta sensibilità al variare del modulo elastico dello stelo.

1. Introduction

A fatigue sensitivity analysis of cemented hip prosthesis is performed in this paper. Human activities generate complex multiaxial stresses varying in time and resulting in the accumulation of mechanical damage in materials and interfaces.
To simulate the fatigue of the cement mantle, a quasi-3D model of the bone-cement implant system is implemented in the finite element code ABAQUS®. The finite element computations provide the principal stresses and directions in every integration points within the cement elements and it is assumed that tensile principal stresses produce a damage perpendicular to that plane [5]. A standard linear damage accumulation rule was showed in a previous paper [1] to predict a strong damage accumulation and a sudden fatigue failure of the cement mantle[6]. A non-linear damage accumulation rule is then introduced to update the tensor which describes the damage produced in the material. A macro-crack is assumed to occur when the damage in a given direction is greater than a threshold value. In that case, a crack is introduced in the material and a standard smeared crack approach is employed [5]. It results in a non-linear, anisotropic behaviour of the locally cracked cement material.
This paper studies the influence of some model parameters such as the cement Young modulus, the stem Young modulus and the bone-cement friction coefficient on the fatigue behaviour of the mantle. In particular the damage distribution and the stem subsidence are investigated.

2. Fatigue damage accumulation model

In the finite element analysis a tensorial damage, $\boldsymbol{D}^{ip}$, is introduced to describe the amount of damage accumulation in the cement mantle in multiple directions in every integration point, *ip*. The bone cement is considered to be elastic and initial isotropic and in the following all the quantities are referred to a given integration points, *ip*.
The presence of the damage implicates some anisotropy of the initially undamaged isotropic cement elements. The principal directions of $\boldsymbol{D}$ determine the directions of the material orthotropy and its principal values, d_I, d_{II}, affect the initial stiffness, $\boldsymbol{S}$, and compliance, $\boldsymbol{C}$, tensors. The stress-strain relationship between the *Cauchy stress*, $\boldsymbol{s}$, and the strain, $\boldsymbol{e}$, tensors in the damaged material is $\boldsymbol{e} = \overline{\boldsymbol{C}} : \boldsymbol{s}$ or $\boldsymbol{s} = \overline{\boldsymbol{S}} : \boldsymbol{e}$ and involves the compliance, $\overline{\boldsymbol{C}}$, and stiffness, $\overline{\boldsymbol{S}}$, tensors of the damaged material. The Cauchy stress tensor is also related to the *effective stress* tensor $\overline{\boldsymbol{s}}$, $\overline{\boldsymbol{s}} = \boldsymbol{M} : \boldsymbol{s}$, through the damage effect tensor $\boldsymbol{M}$ [2] [4]. The complementary elastic energy equivalence hypothesis, $W^e(\boldsymbol{s},\boldsymbol{D}) = W^e(\overline{\boldsymbol{s}})$, is then invoked to define, after replacing the Cauchy stress by the effective one, the elastic compliance tensor $\overline{\boldsymbol{C}} = \boldsymbol{M}^{\mathrm{T}} : \boldsymbol{C} : \boldsymbol{M}$. Finally, the stiffness matrix, $\overline{\boldsymbol{S}}$, of the damaged material is evaluated as the inverse of the compliance tensor, $\overline{\boldsymbol{S}} = \overline{\boldsymbol{C}}^{-1}$. Making use of the undamaged isotropic elastic stiffness matrix for the plane stress situation, the stiffness matrix for the damaged material can be calculated as:

$$\overline{\boldsymbol{S}} = \frac{E}{1-\boldsymbol{u}^2} \begin{bmatrix} (1-D_I)^2 & \boldsymbol{n}(1-D_I)(1-D_{II}) & 0 \\ \boldsymbol{n}(1-D_I)(1-D_{II}) & (1-D_{II})^2 & 0 \\ 0 & 0 & \frac{1-\boldsymbol{u}}{2}(1-D_I)(1-D_{II}) \end{bmatrix} \qquad (2)$$

where E and $\boldsymbol{u}$ denote the Young modulus and the Poisson coefficient of the initially undamaged isotropic material.

It is assumed that the current damage due to a load cycle is governed by the amplitudes, $\boldsymbol{Ds}$, of the principal stress, $\boldsymbol{s}$ = [s_{I}, s_{II}], generated by the loading in a material element [5]. The damage induced anisotropy is described by the compliance, $\overline{\boldsymbol{C}}$, or stiffness, $\overline{\boldsymbol{S}}$, tensors that have to be taken into account while looking for the stresses generated by a maximum and minimum of the loading cycle. Assuming the principal directions of the stress tensor to be unchanged during the following load cycles [2], the amplitudes of the Cauchy principal stresses, $\boldsymbol{Ds}$ = [Ds_I , Ds_{II}], in every integration point are evaluated. The evaluation law of the damage tensor in the principal stresses co-ordinate system is written as follows [2]:

$$\dot{d}_{11} = \frac{1}{c_0 \cdot (m+1)} \cdot \left(\frac{Ds_I}{1-D} \right)^m \qquad \dot{d}_{22} = \frac{1}{c_0 \cdot (m+1)} \cdot \left(\frac{Ds_{II}}{1-D} \right)^m \qquad \dot{d}_{12} = 0 \tag{3}$$

where c_0 and m are the material parameters of the S-N curve and the time derivative is referred to the number of cycles, N, by assuming one cycle as time unit. Integrating Eq. (3), with reference for example to the first diagonal term d_{11} of the damage tensor, over the interval $N \in [0,n]$ provided that $d_{11} = d_{11}^{old}$ at $n=0$ and $d_{11} = d_{11}^{new}$ at $N=n$, one obtains the number of stress cycles $n=N_1$ which augments the damage intensity up to $d_{11} = d_{11}^{new}$:

$$d_{11}^{new} = 1 - \sqrt[m+1]{(1-d_{11}^{old})^{m+1} - \frac{Ds_I^{\;m}}{c_0} \cdot n} \tag{4}$$

$$n = c_0 \cdot Ds_I^{\;m} \cdot (1-d_{11}^{old})^{m+1} \left[1 - \left(\frac{1-d_{11}^{new}}{1-d_{11}^{old}} \right)^{m+1} \right] \tag{5}$$

Similar expressions hold for the other principal stress direction while $d_{12}^{new} = d_{12}^{old}$. These relations are used to update the damage tensor in the principal stress co-ordinate system after the application of a given number, n, of duty cycles. Note that by inserting in Eq. (5) $d_{11}^{old} = 0$ and $d_{11}^{new} = 1$ one recovers the standard one dimension S-N law with reference to the first principal stress direction.

The number of cycles to failure, n_F^{ip}, in the ip integration points is then computed by requiring that one of the principal value of the updated damage tensor is equal to one. The same analysis as described above is performed for all integration points involved in the finite element analysis. The number of cycles to failure in the current increment, NCF, is then computed [5] as $NCF = \min_{ip} \{ n_F^{ip} \}$. The corresponding direction is assumed to be critical and a crack is introduced in the plane perpendicular to such a direction. The updated components of the damage tensor at the end of the increment at each integration points are then computed according to Eqs. (4) by substituting n by NCF. In order to proceed with finite element calculation the stiffness matrix of the damaged elements is updated according to Eq. (2).

3. Implant finite element model

A quasi-3D finite element model (fig. 1a) of a cemented hip prosthesis was created to reduce the computational efforts. The "standardised femur" used in this paper is the computer geometry model of a femoral bone analogue developed by the Laboratory for Biomaterials Technology of Istituti Ortopedici Rizzoli, Italy, within the frame of the Prometeo Project. The femoral analogue is produced by the Pacific Research Labs (Vashon Island, Washington, USA). The model includes a stem-cement interface and a fibrous tissue layer along the cement bone interface with a stiffness reduction by a factor 100 [5]. The side-plate concept [1] is used in order to account for the three-dimensional structural integrity of the cement and cortical bone. The circumferential stresses are recovered by the model as membrane stresses in the corresponding side plate and produce radially directed longitudinal cracks in the cement. The unknown geometric parameters to be calibrated are the cement mantle and cortical bone thickness and the cement and cortical bone side plate thickness (see fig. 1b). These parameters are selected by the following criteria: a) the moment of inertia of the cortical bone and cement section must be equal to those of the real structure; b) the circumferential stresses produced by the simplified elastic theory model reported in fig. 1c must be equal to the membrane stresses in the corresponding side-plate. The internal pressure, *p*, in Fig. 1b comes from the finite element analysis as normal stresses in the stem-cement interface.

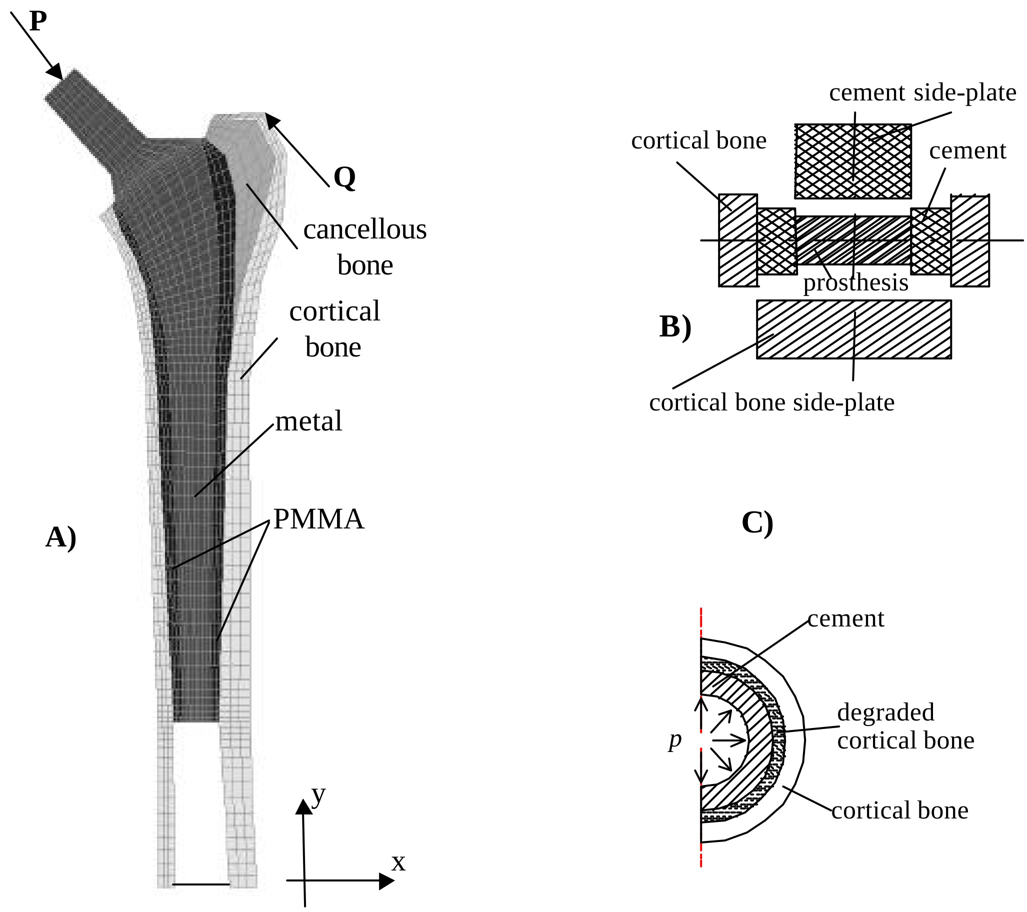

Fig. 1. a) front plane of the finite element mesh; b) the non-uniform thickness section of the model; c) elastic theory model used to calibrate cortical and cement thickness.

4. Results

The finite element calculations involved in the fatigue damage evaluation were performed by the finite element code ABAQUS®. A custom made procedure was developed to read the stresses at the integration points at the end of each increment and to evaluate the number of cycles to create a new fracture in the cement mantle (see section 2). Finally, a user subroutine was inserted to evaluate the element stiffness matrix of the damaged elements. The model contains 2384 4-nodes plane stress elements and 2824 nodal points. The simulated loading case (see fig. 1a) was the one generated during the stance phase of walking at 6 *Km/h* [1] with a force *P* of 3250 *N* acting on the prosthetic head, with an angle of 12° on the vertical axis. Muscles forces *Q* were assumed acting on the greater trochanter with a total intensity of 2250 *N* and an inclination on the vertical axis equal to 12°. This load was assumed to be applied to structure repeatedly, in cycles from zero to the maximum value. In this paper the *S-N* relationship proposed in [3] is adopted:

$$log(n_F) = -m \cdot log\, \Delta\sigma_i^{ip} + log\, c \tag{6}$$

with material parameters m = 4.68 and log c = 8.77 (MPa units).
The sensitivity analysis is performed with reference to the stem subsidence and the damage level in the cement mantle, $D_{tot}(n)$:

$$D_{tot}(N) = \sum_{ip=1}^{IP} \sum_{i=1}^{2} D_i^{ip}(n) \tag{7}$$

The analyses take place changing one model parameter each time while keeping the other ones unchanged. The considered model parameters are the cement Young modulus, the stem-cement friction coefficient and the femoral component Young modulus (see tab. 1). Moreover, two different materials are considered for the femoral component: titanium Ti-6Al-4V alloy (Young modulus equal to 110 GPa) and steel Cr-Co-Mo alloy (Young modulus equal to 205 GPa). The base value considered for each parameter is the central value of the interval in tab. 1 and titanium stem. The Young modulus of the cortical bone is equal to 18.6 GPa is not taken into account in the sensitivity analysis. The bone was assumed to be linear elastic and isotropic with constant in time mechanical properties.
The results of the sensitivity analysis are reported in figs. 2-3 and 4. In these figures the black circles indicate the failure point on the corresponding curve. The fatigue failure of the implant is defined as the complete development of a crack, from the distal to the proximal end, in the cement side plate.

Table 1. Numerical values of the parameters considered in the sensitivity analysis.

Parameter	Numerical values
Bone cement Young modulus	2.0 – 2.2 – 2.4 GPa
Stem Young modulus	110 – 205 GPa
Stem-cement friction coefficient	0.2 - 0.3 - 0.35

Consider first the variation of the total damage and stem subsidence as function of the cement Young modulus. The fatigue lifetime corresponding to a cement Young modulus of 2.2 Gpa (the base value in tab. 1) is equal to $6.96 \cdot 10^6$ duty cycles. A reduction of the bone cement

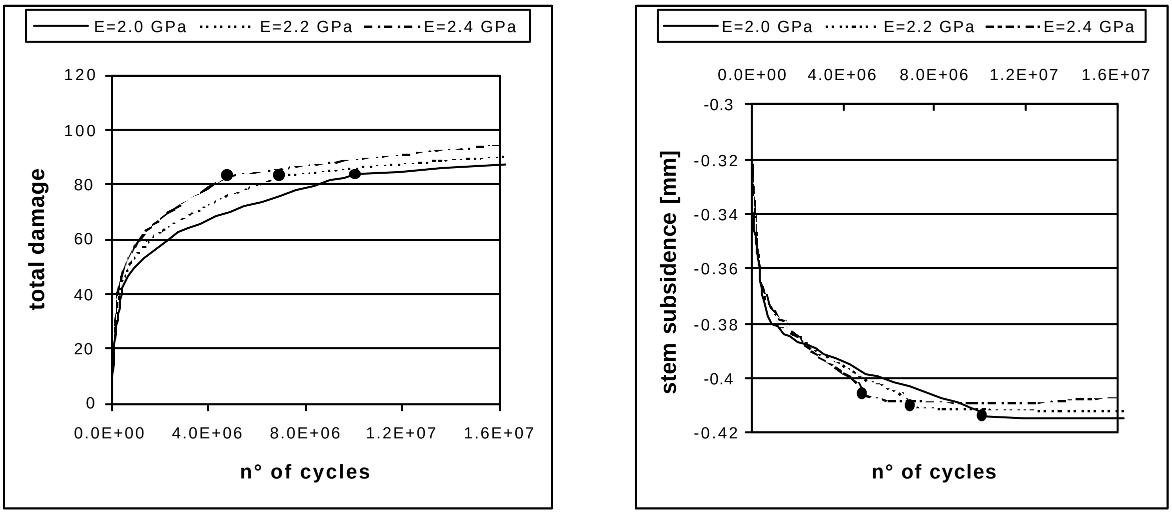

Figure 2. Total damage and stem subsidence vs. cement Young modulus.

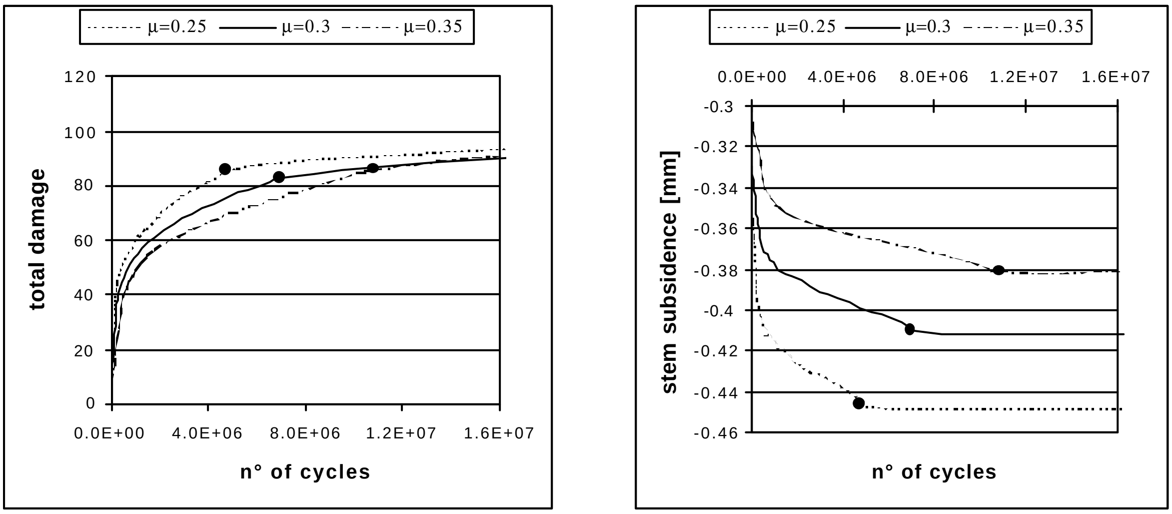

Figure 3. Total damage and stem subsidence vs. stem cement friction coefficient m

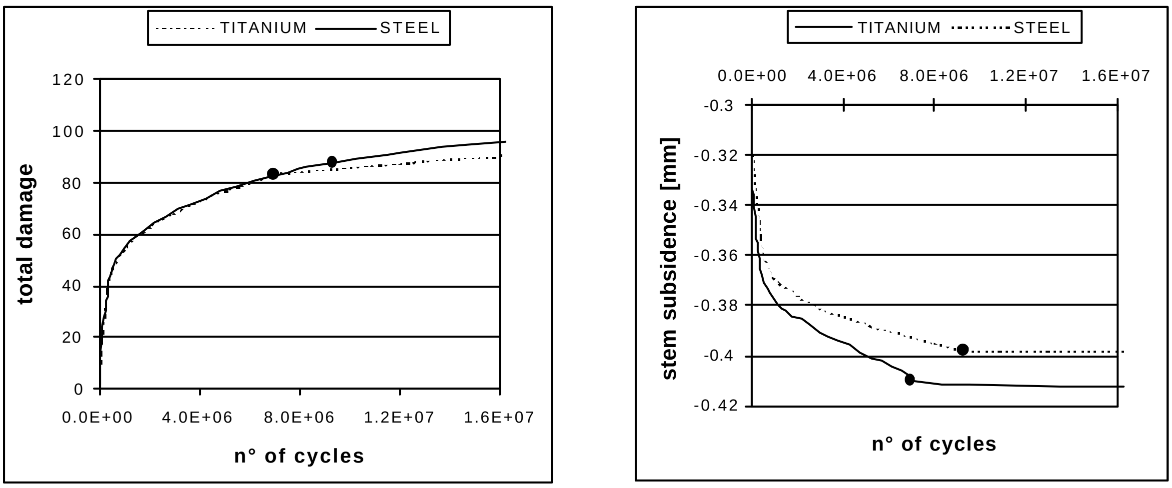

Figure 4. Total damage and stem subsidence vs. different stem Young modulus.

modulus produces an increment (44%) of the fatigue lifetime (see fig. 2) up to $10.07 \cdot 10^6$ duty cycles. In fact, due to the stiffness reduction corresponding to a lower modulus, the circumferential stress level in the cement mantle is reduced while the cortical bone one is increased and, as a consequence, a lower damage level is achieved in the cement. On the contrary, an increment of the bone cement modulus leads to an increment of the stiffness and then to lower stresses and damage level. As a consequence a reduction (30%) of the fatigue lifetime is achieved up to $4.85 \cdot 10^6$ duty cycles. On the other hand, the variation of the bone cement Young modulus produces only marginal variations to the stem subsidence (see fig. 2) with values ranging from -0.406 mm to -0.414 mm. Note that a very small variation of the stem subsidence produces a significant variation of the fatigue lifetime.
Consider second the variation of the total damage and stem subsidence as function of the stem-cement friction coefficient. The fatigue lifetime corresponding to a friction coefficient equal to 0.3 (the base value in tab. 1) is again equal to $6.96 \cdot 10^6$ duty cycles. An increment of the friction coefficient produces a significant increment (55%) of the fatigue lifetime (see fig. 3) up to $10.85 \cdot 10^6$ duty cycles. In fact, an increment of the bonding between the femoral component and the cement reduces the circumferential stresses and then the damage level and gives rise to a greater fatigue lifetime. On the contrary a reduction of the friction coefficient leads to an increment of the stress and damage level and then a significant reduction (32%) of the fatigue lifetime. This effect is also evident from the point of view of the stem subsidence. The reduction of the friction coefficient leads to an increment (9%) from -0.408 mm to -0.446 mm of the stem subsidence. On the contrary, an increment of the friction coefficient produces a reduction (7%) from -0.408 mm to -0.381 mm of the stem subsidence. This clearly shows the very high sensitivity of the fatigue lifetime to stem subsidence.
Consider finally the variation of the total damage and stem subsidence as function of the femoral component Young modulus. The shear stresses at the stem-cement interface are positively correlated with the ratio between the stem and cement Young modulus. A steel femoral component gives rise then to higher shear stresses at the stem-cement interface compared to the titanium stem (the base case in tab. 1). This produces a reduction of the stem subsidence (see fig. 4) and then a lower stress and damage level in the cement mantle (remember that an increment of the stem subsidence gives rise to an increment of the circumferential stresses which are responsible of micro-cracks development and growth). The titanium femoral component subsidence is equal to -0.408 mm while the steel femoral component subsidence is equal to -0.398 with then a small decrement (2.5%). The fatigue lifetime (see fig. 4) is again equal to $6.96 \cdot 10^6$ duty cycles in the titanium stem case and it increases to $8.24 \cdot 10^6$ duty cycles in the steel case with a significant increment (18%). This shows again that the fatigue lifetime is very sensitive to stem subsidence.

5. Discussion

A quasi-3D model is introduced in this paper to study the damage evaluation in the cement mantle of a prosthesis implant. This study addresses the damage accumulation failure scenario with respect to the cement mantle [6]. However, the long term lifetime is governed by biological factor such as debris effects and particulate reactions.
The damage accumulation [1] is governed by the bending stresses in the bounded stem-cement interface case and by the circumferential stresses in the unbounded case. The unbounded stem-cement case was found [1] to produce a larger damage level compared to the bounded one. This is because the circumferential stresses in the unbounded situation are greater than bending stresses in the bounded case. In this paper only the more realistic and conservative situation of unbounded

stem-cement interface is then considered. In this paper a more realistic continuous damage model compared to the one in [1] and [5] is implemented. In particular a non-linear damage accumulation rule is introduced and the elements stiffness matrix are updated at the end of each increment. In fact, stress redistribution due to cement damage reduces the damage rate in time and increases the fatigue lifetime and must be taken into account in a realistic analysis.
The fatigue lifetime is sensitive to the bone cement Young modulus. In fact, an increment of the stiffness of the bone cement produces an increment of the circumferential stresses in the cement mantle and then a reduction of the fatigue lifetime. However, the stem subsidence remains unchanged because the shear stresses at the interface are not influenced by a variation of the cement modulus. The analyses show that the fatigue lifetime is very sensitivity to the stem-cement friction coefficient. Clearly, a firm and last bonding between the stem and the cement mantle reduces the stem subsidence and then the damage level, although it is difficult to realise clinically. A stem design with flanges or collars may lead to less subsidence and then to a greater fatigue lifetime. Finally, the steel femoral component behaves better than the titanium one with respect to the damage accumulation in the cement mantle.

Acknowledgement

The financial support from the Milan Technical University to the first author and from the State Committee for Scientific Research under the grant N° 8 T11F 017 18 to the second author is gratefully acknowledged.

References

[1] Colombi P., Dolinski K., "*Fatigue Analysis of Cement Mantle After Total Hip Arthroplasty*", Atti del XIV Congresso AIMETA, Como 6-9 Ottobre, **1999**.

[2] Dolinski K., "*Fatigue damage and reliability assessment of cemented hip prosthesis*", Journal of Theoretical and Applied Mechanics, **37 (3)**, 505-518, **1999**.

[3] Davies J.P. et al., "*Comparison of the fatigue characteristics of the centrifuged and uncentrifuged Simplex P bone cement*", Journal of Orthopaedic Research, **5**, 366-371, **1987**.

[4] Lu T.J., Chow C.L., "*On constitutive equations of inelastic solids with anisotropic damage*", Theoretical and Applied Fracture Mechanics, **14**, 187-218, **1990**.

[5] Verdonschot N., Huiskes R., "*The effects of cement-stem debonding in THA on the long-term failure probability of cement*", Journal of Biomechanics, **30 (8)**, 795-802, **1997**.

[6] McCormack B.A.O. and Prendergast P.J., "*Microdamage accumulation in the cement layer of hip replacements under flexural loading*", Journal of Biomechanics, **32**, 467-475, **1999**.